Local modulation of the Wnt/β-catenin and BMP pathways recapitulates rib defects analogous to cerebro-costo-mandibular syndrome

Benedict R H Turner and Nobue Itasaki

Faculty of Health Sciences, University of Bristol, Bristol, BS2 8EJ, UK

Corresponding:

Benedict R H Turner

Centre for Applied Anatomy, Faculty of Health Sciences, University of Bristol

Southwell Street, Bristol, BS2 8EJ, UK

bt14988@bristol.ac.uk

Abstract

Ribs are seldom affected by developmental disorders, however, multiple defects in rib structure are observed in the spliceosomal disease cerebro-costo-mandibular syndrome (CCMS). These defects include rib gaps, found in the posterior part of the costal shaft in multiple ribs, as well as missing ribs, shortened ribs and abnormal costotransverse articulations, which result in inadequate ventilation at birth and high perinatal mortality.

The genetic mechanism of CCMS is a loss-of-function mutation in *SNRPB*, a component of the major spliceosome, and knockdown of this gene *in vitro* affects the activity of the Wnt/β-catenin and BMP pathways. This study aims to investigate whether altering these pathways *in vivo* can recapitulate rib gaps and other rib abnormalities in the model animal. Chick embryos were implanted with beads soaked in Wnt/β-catenin and BMP pathway modulators during somitogenesis and incubated until the ribs were formed. Some embryos were harvested in the preceding days for analysis of the chondrogenic marker *Sox9,* to determine whether pathway modulation affected somite patterning or chondrogenesis.

Wnt/β-catenin inhibition manifested characteristic rib phenotypes seen in CCMS, including rib gaps ($P<0.05$) and missing ribs ($P<0.05$). BMP pathway activation did not cause rib gaps but yielded missing rib ($P<0.01$) and shortened rib phenotypes ($P<0.05$). A strong association with vertebral phenotypes was also noted with BMP4 ($P<0.001$), including scoliosis ($P<0.05$); a feature associated with CCMS. Reduced expression of *Sox9* was detected with Wnt/β-catenin inhibition, indicating that inhibition of chondrogenesis precipitated the rib defects in the presence of Wnt/β-catenin inhibitors. BMP pathway activators also reduced

Sox9 expression indicating an interruption of somite patterning in the manifestation of rib defects with BMP4.

This study demonstrates that local inhibition of the Wnt/β-catenin and activation of the BMP pathway can recapitulate rib defects such as those observed in CCMS. The balance of Wnt/β-catenin and BMP in the somite is vital for correct rib morphogenesis, and alteration of the activity of these two pathways in CCMS may perturb this balance during somite patterning leading to the observed rib defects.

Keywords: Cerebro-costo-mandibular syndrome (CCMS), Wnt, BMP, rib gap, rib defects, somite patterning, chondrogenesis, epaxial, hypaxial

Introduction

The rib is an anatomically unique structure: by articulating with the vertebrae in distinct ways, the ribs form a cage that is flexible enough to allow ventilation but strong enough to protect the internal organs. Defects in rib structure are rare, implying a robust mechanism that is resilient to congenital errors in development. Yet, one example of a condition in which multiple defects in rib structure are observed is cerebro-costo-mandibular syndrome (CCMS). First characterised in 1966, CCMS is a developmental disease with craniofacial and rib defects including rib-gaps, missing ribs, abnormal costo-transverse articulations and shortened ribs (Smith et al., 1966). Of these, the most remarkable is the presence of rib gaps, a discontinuity occurring in the proximal part of the costal shaft of multiple ribs. The finding is pathognomonic of CCMS and results in perinatal instability of the thoracic cage, leading to extensive medical intervention and high mortality (Tooley et al., 2016, Watson et al., 2014).

Two groups have independently confirmed that loss-of-function mutations in small nuclear ribonuclear associated protein B/B' (*SNRPB)* cause CCMS. *SNRPB* encodes a component of the major spliceosome SmB/B' and mutation leads to inclusion of a premature termination codon that reduces the protein level (Bacrot et al., 2015, Lynch et al., 2014). *In vitro,* downregulation of *SNRPB* expression results in a reduction of inclusion of alternative exons in hundreds of genes (Saltzman et al., 2011), however, it is not known how reduction in a component of the major spliceosome affects skeletogenesis.

In early embryogenesis after gastrulation, the paraxial mesoderm undergoes metameric segmentation to form somites, which give rise to the axial skeleton, skeletal muscles and dorsal dermis (Bothe et al., 2007). The somite is patterned

along its dorsoventral and mediolateral axes to form four discrete compartments known as the dermomyotome, myotome, syndetome and sclerotome (Bothe et al., 2007, Brent et al., 2003). The sclerotome is the most ventral compartment in the somite and embryological antecedent of the axial skeleton (Huang et al., 2000, Evans, 2003). Soluble ligands from the surrounding tissues stimulate cell fate commitment, proliferation, migration and differentiation of sclerotome cells to form axial structures such as the ribs and vertebrae. Three well known pathways involved in somite patterning and skeletal development are the bone morphogenic protein (BMP), Wnt/β-catenin (referred to as Wnt in this paper) and sonic hedgehog (Shh) pathways (reviewed in (Bothe et al., 2007, Geetha-Loganathan et al., 2008). For rib phenotypes to occur, it is hypothesised that the process of somite patterning may be disrupted through altered balance of at least one of these pathways.

Dorsoventral patterning of the somite precedes growth and differentiation of cartilage and bone progenitors in the sclerotome (Huang et al., 2000, Evans, 2003). This occurs through secretion of Shh and the natural BMP inhibitor Noggin from the notochord and floor plate of the ventral neural tube (McMahon et al., 1998, Marcelle et al., 1997). Noggin antagonises BMP signals that emanate from the lateral plate mesoderm and dorsal neural tube (Pourquie et al., 1996, Tonegawa et al., 1997). Secretion of these signalling molecules generates a concentration gradient of Shh from ventral to dorsal and an opposing gradient of BMP pathway activity, eliciting different somitic cell fates at given concentrations (Fan and Tessier-Lavigne, 1994, Johnson et al., 1994, McMahon et al., 1998, Cairns et al., 2008). High concentrations of both Shh and Noggin are required for induction and maintenance of the sclerotome markers *Pax1* and *Pax9* in the

ventromedial somite, which suppress myotome and dermomyotome markers (Muller et al., 1996, Balling et al., 1988, McMahon et al., 1998, Furumoto et al., 1999, Cairns et al., 2008). *Pax1* is first broadly expressed in the sclerotome and gradually confined to the most ventromedial part of the somite, where it induces *Pax9* expression. *Pax1* mutants and *Pax1/Pax9* double homozygous mutants both fail to form the proximal rib, including the head, neck and tubercle, as well as the vertebra (Wallin et al., 1994, Dietrich and Gruss, 1995, Balling et al., 1988, Peters et al., 1999). Together, these ventral sclerotome derivatives are known as the epaxial skeleton and are Pax1-dependent (Brand-Saberi et al., 1993, Koseki et al., 1993, Wallin et al., 1994, Christ et al., 2004). On the other hand, the lateral half of the somite is specified mainly by BMP signals, of which the sclerotomal portion develops into the distal rib (Pourquie et al., 1996, Stafford et al., 2011, Olivera-Martinez et al., 2000). In both *Pax1/9* mutants and CCMS, the distal rib is kept intact. However, the rib defects observed in *Pax1 and Pax1/9* mutants differ from the CCMS phenotype, as the vertebrae and proximal ribs fail to develop rather than forming a gap in the costal shaft. As such, the rib defects in CCMS are unique and likely caused by multiple gene defects at various developmental stages.

In addition to somite patterning, the Wnt and BMP pathways are intimately involved in the growth and differentiation of cartilage and bone (reviewed in (Itasaki and Hoppler, 2010). BMPs were originally named for their ability to stimulate cartilage and bone growth (Wozney et al., 1988), and BMP2 promotes chondrogenesis through induction of *Sox9* expression (Yoon and Lyons, 2004, Pan et al., 2008). The Wnt pathway positively regulates osteogenic activity (Holmen et al., 2005) and, together with the BMP pathway, cooperates for

osteochondrogenesis (Fischer et al., 2002, Mbalaviele et al., 2005, Chen et al., 2007). Knockdown of *SNRPB in vitro* demonstrated that Wnt pathway activity was significantly decreased and BMP pathway activity was significantly increased in HEK293 cells (Unpublished). The roles of these signals in sclerotome development and cartilage formation are well known and summarised above, but little is known about the impact of signal modulation on rib development.

Here, we show that local modulation of the Wnt, BMP and Shh pathways causes a wide variety of rib and vertebral defects in chick embryos. Most striking of all was the recapitulation of the rib gap phenotype, that has never before been seen in model animals, through local inhibition of the Wnt pathway. Other defects seen in CCMS such as missing ribs, scoliosis and shortened ribs were also observed with activation of the BMP pathway and inhibition of the Wnt pathway. The expression pattern of *Sox9* as a marker of chondrogenic differentiation in somites (Lefebvre et al., 1997, McKeown et al., 2005) suggested that rib gaps were mainly due to the effect of Wnt inhibitors on chondrogenesis, whilst BMP pathway activation affected dorsoventral patterning. We propose that the manifestation of rib abnormalities in CCMS is due to a combination of disrupted dorsoventral patterning of somites and inhibition of chondrogenic differentiation.

Methods

Egg incubation

Chick embryos were used as a model system because of the accessibility of somites and capacity to continue incubation after the intervention. Fertilised chick eggs were incubated at 38°C in a horizontal position to allow the embryo to

surface to the superior aspect of the yolk. Incubation for around 50 hours yielded a range of embryos from Hamburger and Hamilton (HH) stage 11-14 (Hamburger and Hamilton, 1951). Eggs were then washed with 70% ethanol, and 3ml of albumen was withdrawn using a sterile syringe and needle. A 2cm oval window was cut into the shell on the superior surface of the horizontal egg, exposing the embryo beneath the amnion and vitelline membrane. After bead implantation, the eggs were sealed with tape and placed back in the incubator for a further 1-12 days.

Bead preparation

Beads were soaked for an hour in pathway activity-modulating chemicals or proteins, before implantation into the embryos. The chemicals used to soak the beads were selected in accordance with their ability to either activate or inhibit the BMP, Wnt and Shh pathways (Table 1). Two types of beads were used in this experiment: heparin beads (Source Biosciences) for BMP4 and Dkk1 proteins and AG 1-X2 (BioRad) beads for inorganic chemicals. The solvent for proteins was phosphate buffered saline (PBS) and for inorganic chemicals was dimethyl sulphoxide (DMSO); concentrations of the soaking solutions can be seen in Table 1. After soaking, the beads were washed in PBS solution. One µl of Fast-Green dye and penicillin (100units/ml) with streptomycin (100µg/ml) was administered on to the vitelline membrane for anatomical visualisation and infection control. The vitelline membrane and amnion were peeled back, and an incision was made on the right side of the thorax between the neural tube and somite or pre-somitic mesoderm in younger embryos, at the level of somites 20-26 from which the chicken ribs develop. This level corresponds to just below the point at which the

umbilical vessels enter the embryo, making them a good marker for the intervention in the absence of somites. Beads were then implanted into the youngest somite of the 20-26 range, or if the embryo was too young to have developed somites in this range then the most cranial part of the pre-somitic mesoderm was used. Based on resegmentation theory, which states that each rib and vertebra are composed from the caudal and cranial hemi-somites (Stern and Keynes, 1987), two beads were implanted across two somite levels. This ensured that an entire rib and vertebra would be exposed to the intervention. Due to the nature of performing a three-dimensional procedure on a two-dimensional field, some of the beads were placed relatively deeper and settled in the ventral portion of the somite, whilst other beads settled dorsally if the incision was more superficial. This resulted in a slight variation of implantation depth which only became apparent once the embryos were fixed for the analysis.

Embryo processing for cartilage and bone staining

Post-incubation, embryos were isolated from the yolk and albumen. The head, abdominal and thoracic organs were dissected out to maximise intensity and clarity of staining. The embryos were fixed in 96% ethanol for 24 hours, before being bathed in 0.02% Alcian blue solution with 70% ethanol and 5% acetic acid for a further 24 hours. Where appropriate 0.005% Alizarin red was also added for bone staining. The soft tissues were then dissolved using 1% potassium hydroxide (KOH) solution and preserved in a glycerol/ KOH mixture (Behringer, 2014).

***In-situ* hybridisation**

Some embryos were harvested 24 hours after bead implantation and processed for *in situ* hybridisation, to evaluate the position of bead implantation and somite patterning. Due to the range of HH stages at implantation, harvesting 24 hours late led to collection of embryos at HH stages 16-18. The *Sox9* probe (kindly gifted by Dr M. Cheung, University of Hong Kong) was used, following the hybridisation protocol (Acloque et al., 2008). Embryos were then embedded in 3% agarose blocks and cut into 50 μm sections using a vibratome.

Statistical analysis

Each chemical or protein was examined in its ability to elicit any one of the thirteen different phenotypes. When compared in their ability to generate the rib phenotypes, the two control beads DMSO and PBS, were not statistically different on any count and, as such, the results of the two controls were combined to create a greater control size.

The number of embryos in the control group displaying a phenotype was less than 5 in most cases. Therefore, a one-tailed Fisher's exact test was employed instead of the Chi-Squared test, to compare the test chemicals and proteins to the controls in their ability to generate each phenotype. Using this method, statistically significant effects of 2-bead implantation were identified as shown in Table 2. After the finding that phenotypes were much more pronounced using two-bead data, the one-bead data were excluded from the statistical analysis in this study.

Results

Classification of phenotypes and statistical analysis

Of a total 116 embryos that survived to be stained for cartilage development analysis, 83 embryos (72%) displayed one or more phenotypes as described below. The incidence of phenotypes by individual chemicals is shown in Table 2 along with classification of the phenotype and statistical analysis. The table highlights how each chemical or protein pathway modulator generated a unique set of typical traits presented in the figure panels below (Fig. 1-4), revealing the effect of Wnt, BMP and Shh pathway modulation on rib and vertebral morphogenesis.

Despite the instructive role of Wnt, BMP and Shh signals in development, the incidence of phenotypes was variable. This may be due to the long re-incubation period that resulted in variable displacement of the beads during morphogenesis, as demonstrated by the range of bead positions in Fig. 1-5. The lower phenotype incidence with increased length of incubation period has also been documented by others performing bead experiments (Huang et al., 2003).

Additionally, whilst the beads were always placed on the right side of the thorax, some left-sided phenotypes did occur. In such embryos, the bead was often found close to the midline in the vertebral column and hence, could affect the contralateral side. This is likely a manifestation of the ventral migration of sclerotome cells and left-sided phenotypes are therefore considered to be due to medial displacement of beads during growth. This is particularly emphasised in the present study, due to the long latency between bead implantation and harvesting.

Phenotypes yielded by Dkk1

Two different Wnt pathway inhibitors, Dkk1 and PNU-74654, were used in this experiment. Dkk1 is a LRP5/6 co-receptor antagonist and hence prevents cellular transduction of Wnt signals (Mao et al., 2001, Semenov et al., 2001). Fig. 1 displays the statistically significant phenotypes observed with Dkk1, which included the presence of rib gaps. Due to the degree of variation in the rib gap phenotype, it was sub-categorised into two further groups: proximal rib defects and shaft defects. The proximal rib defect is defined as absence of the costal head, neck and/or tubercle, often associated with structural underdevelopment of the vertebra (Fig. 1A,D,F). Whereas, a shaft defect is defined as a discontinuity within the rib shaft with preserved rib head and neck (Fig. 1B,C). For both shaft defects and proximal rib defects, the phenotype was statistically significant ($P<0.05$).

Other typical phenotypic features for Dkk1 compared to other chemicals, were that it had a higher incidence of multiple rib gaps at different axial levels (Fig. 1A,C,D) and frequently had associated vertebral phenotypes (Fig. 1A,D-G). These included vertebral malformations ($P<0.05$) which is any alteration to the normal vertebral morphogenesis such as hemi-vertebrae, as well as vertebral fusions, where a vertebra becomes fused to its cranial or caudal counterpart (Fig. 1A, D-G). Other skeletal defects observed included the incidence of missing ribs ($P<0.01$), defined as the lack of the entire length of a rib (Fig. 1E-H), and shortened ribs, which are truncations of the distal part of the rib that reduce its overall length (Fig. 1E).

Phenotypes yielded by PNU-74654

PNU-74654 is a small molecule inhibitor of the Wnt pathway that blocks intracellular β-catenin interactions (Trosset et al., 2006). Fig. 2 displays the phenotypes observed with PNU74654 and, as with Dkk1, both the shaft defect (Fig. 2A-D) and proximal rib defect (Fig. 2E-G) phenotypes were significant ($P<0.05$), yet there were subtle differences between PNU-74654 and Dkk1. Chiefly, rib gaps were noted to be larger with PNU-74654 than Dkk1, and occurred at a single axial level (Fig. 2A,C,D). Other differences with PNU-74654 beads as compared to Dkk1 included additional pairs of ribs, less common vertebral phenotypes and fewer instances of missing ribs (Fig. 2E-H; Table 2).

Phenotypes yielded by BMP4

As would be expected, placing BMP4 into the paraxial mesoderm of the developing embryo had a profound effect on rib and vertebral development, with the most extreme examples seen in Fig. 3A-D. Principally affected in these embryos was vertebral development, with trans-sectional fusion of vertebrae across many axial levels (Fig. 3A,D,H) ($P<0.001$), marked serial vertebral maldevelopment (Fig. 3B,D,G) ($P<0.001$) and scoliosis (Fig. 3A,C,D) ($P<0.05$), a three-dimensional deformity of the spine with curvature and rotation. However, these cases of scoliosis exhibited marked vertebral malformation and fusion, thus, the phenotype presented here is due to developmental failure of the vertebrae. This differs from the phenotype in CCMS patients, who develop scoliosis during childhood (Tooley et al., 2016).

Another key element to the BMP4 phenotype was missing ribs (Fig. 3A-D,F,G), which occurred almost as frequently as vertebral phenotypes ($P<0.01$). Furthermore, shortened ribs (Fig. 3B,G) ($P<0.05$), a truncated version of the rib

297 that has intact proximal rib elements with variable length at distal segments, were
298 also noted with BMP4. Rib fusions, the joining of two adjacent ribs to one another
299 (Fig. 3C,F-H), and rib malformations, any structural abnormality in the form of the
300 rib excluding shortening, bifurcation, fusion or rib gaps, were also observed (Fig.
301 3A,D) ($P<0.05$) but intriguingly rib gap defects were seen sparingly in this group
302 (Fig. 3E,F).
303
304 **Phenotypes yielded by K02288**
305 K02288 is a selective inhibitor of type I BMP receptors (Sanvitale et al., 2013).
306 Embryos implanted with K02288 beads only displayed defects that were highly
307 localised to the position of the bead (Fig. 4). The defining feature was the high
308 frequency of rib fusions (Fig. 4A-D,F) ($P<0.01$) as well as vertebral fusions limited
309 to two adjacent vertebrae (Fig. 4A-C,E,G,H) ($P<0.001$) and focal vertebral
310 defects (Fig. 4B,E,G,H) ($P<0.01$), that all occurred in close proximity to the bead.
311 This is in direct contrast to BMP4, which generated profound malformations
312 affecting the entire vertebra, often across multiple axial levels. In addition,
313 missing ribs were noted with K02288 beads ($P<0.05$), though in most cases this
314 appeared to be due to fusion of two ribs to one another (Fig. 4B-E). Thus, whilst
315 the table shows that similar traits were caused by BMP pathway activation and
316 inhibition, Fig. 3 and 4 display how the manifestation of these phenotypes is very
317 different (see Discussion).
318
319 **Phenotypes yielded by other chemicals**
320 Fig. 5 presents a summary of the typical defects generated by cyclopamine, BIO
321 and DMSO. Defects caused by the Shh inhibitor cyclopamine (Incardona et al.,

1998) were mostly rib and vertebral fusions (Fig. 5A) as well as vertebral bridging, small cartilaginous projections joining the inferolateral corner of the superior vertebra with the transverse process of the inferior vertebra (Fig. 5B). However, none of these phenotypes achieved statistical significance. BIO (Meijer et al., 2003), was expected to yield phenotypes because of its strong activation of the Wnt/β-catenin pathway, but only generated rib malformations ($P<0.05$) (Fig. 5C,D).

The two control solvents used in this study were PBS and DMSO. Similar to results described in other studies (Nifuji et al., 1997), the controls demonstrate that the beads themselves can cause ectopic cartilage production and rib bifurcation (Table 2; Fig. 5E,F). Likely, this is due to the physical intervention causing disruption of cell condensations resulting in a small group of cells being split from the main chondrogenic population.

Sox9 expression implicates pathway modulation in somite patterning and chondrogenesis

To determine whether the pathway modulators acted on dorsoventral patterning of the somites or chondrogenesis, the chondrogenic cell fate marker *Sox9* was used on embryos harvested one day after bead implantation. Expression of *Sox9* is first broad in the whole somite and later localised to the chondrogenic precursors in the sclerotome (Lefebvre et al., 1997, McKeown et al., 2005). It is therefore considered that *Sox9* indicates the cells' potency to undergo chondrogenic differentiation. The pathway modulators used in the beads were BMP4, Dkk1 and PNU-74654 due to implication of BMP pathway activation and Wnt pathway inhibition in *SNRPB* knockdown cells (unpublished). It was

observed that all three reagents reduced *Sox9* expression in the developing sclerotomes (Fig. 6). This result was interpreted with the known effects of the Wnt and BMP pathways on dorsoventral patterning of the somite and chondrogenesis, the significance of which is discussed below.

Discussion

The remarkable rib gap phenotype is one of the defining features of CCMS and has here been reliably replicated by local inhibition of the Wnt pathway through bead implantation. The mechanism through which Wnt inhibitors may exert this effect relies on two separate roles of the Wnt pathway during skeletal development; dorsoventral patterning of the somite and chondrogenesis.

Somite patterning and proximal rib development

Wnt signals are secreted by the roof plate of the neural tube and surface ectoderm, inducing dermomyotome formation in the dorsal somite through *Pax3, Myf5 and MyoD* expression (Capdevila et al., 1998, Ikeya and Takada, 1998, Otto et al., 2006). Together with the ventralising signal Shh, dorsoventral patterning of the somites is achieved. However, it has been shown that genetic knockout of Wnt3a does not affect development of the sclerotome, rather, it only reduces the dermomyotome (Ikeya and Takada, 1998). In addition, the fact that the Wnt pathway is not active in the sclerotome during the early stages of somitogenesis, supports that Wnt signalling is not required for sclerotome development (Qian et al., 2011). Therefore, it is likely that Wnt inhibitors administered in the medial side of the somite would not impact dorsoventral patterning, for if they had, then expansion of the ventral domain of the somite would have been anticipated, which was not observed (Fig. 6A,B). Hence, reduced Sox9 expression in somites due to Wnt inhibitors suggests differentiation of chondrocytes was affected, rather than dorsoventral patterning.

However, it is unclear why CCMS patients do not present with myotomal phenotypes if the Wnt pathway is affected. In fact, the Wnt pathway is required in

many aspects of embryogenesis such as gastrulation, neurulation and organogenesis, none of which are affected in CCMS. Therefore, it is speculated that the defect in the Wnt pathway is rather mild *in vivo* and additional mechanisms likely regulate the localised phenotype.

Different from the dorsoventral axis, the mediolateral axis of the somite is patterned mainly by BMP signals from the intermediate and lateral plate mesoderm. Along with the endogenous BMP antagonist Noggin from the notochord, a gradient of BMP activity is created, from low at the medial to high at the lateral side of the somite (Pourquie et al., 1996, Tonegawa et al., 1997, Tonegawa and Takahashi, 1998). High BMP signals induce *Sim1* expression in the lateral half of the somite, thus dividing it into epaxial and hypaxial domains mediolaterally (Pourquie et al., 1996, Cheng et al., 2004). The epaxial (medial) portion of the sclerotome, which is *Pax1*-positive and Sim1-negative, gives rise to the ipsilateral vertebra and proximal rib; the costal head to the costal angle (Bothe et al., 2007, Cheng et al., 2004, Olivera-Martinez et al., 2000), and is delimited by the attachment of the epaxial muscles at the costal angle (Moore et al., 2014). In CCMS, it appears from clinical images that the rib gaps centre around the angle of the rib at the epaxial-hypaxial border (Doyle, 1969, Silverman et al., 1980, Tachibana et al., 1980, Plotz et al., 1996, Watson et al., 2014, Tooley et al., 2016). It is hence speculated that unbalanced BMP signals are involved in the rib gap phenotype in CCMS, through the perturbation of the mediolateral patterning of the somite.

In this study, both BMP4 and the BMP receptor inhibitor K02288 affected rib morphogenesis, with distinct phenotypes (Figs. 3 and 4). Exogenous BMP4 introduced by bead implantation into the medial side of the somite has likely

hindered development of the medial somite by antagonising Noggin. This diminishes the epaxial domain, resulting in defects in derived structures such as the vertebrae and proximal ribs, as seen in Fig. 3. These phenotypes are similar to those caused by deletion of *Pax1/9* (Wallin et al., 1994) or by excess BMP signals (Stafford et al., 2011, Stafford et al., 2014, Tonegawa et al., 1997). They are due to a failure of sclerotome specification, reflected by reduced expression of *Pax1* in the ventral somite (Tonegawa et al., 1997, Stafford et al., 2011, Stafford et al., 2014) that subsequently causes a failure of maintaining *Sox9* (Peters et al., 1999) which was also observed in this study (Fig. 6D). The high BMP signals in this study therefore most likely affected the normal gradient of BMP signals from medial to lateral across the somite, thus affected the entire epaxial sclerotome causing the vertebral and rib defects (Fig. 3). The report that exogenous BMP2 is able to induce rib abnormalities in chicks on embryonic day two (HH stage 12) but not day three (HH stage 19) (Nifuji et al., 1997), agrees with our result and suggests that the somites are patterned by the end of embryonic day 2.

K02288 beads produced focal rib and vertebral defects including missing ribs, vertebral malformations and vertebral fusions, localised to the bead position. In somite patterning, K02288 may be anticipated to expand the epaxial domain, in contrast to BMP4. However, the endogenously expressed Noggin already functions as a BMP inhibitor, therefore additional BMP inhibitor was likely not effective in somite patterning. Furthermore, given that K02288 is a chemical compound and likely more stable than BMP4 proteins, it is speculated that the chemical persisted till later stages of development to affect cartilage differentiation. This is concordant with the observation that the defects with

K02288 were localised to the bead location. That is to say, despite the possible expansion of the medial sclerotome, the cells fail to differentiate into cartilage as BMP signals are crucial for chondrogenesis (Yoon and Lyons, 2004). Therefore, K02288 is able to cause skeletal defects through interruption of chondrogenesis.

Somite patterning and position of the rib gap

As mentioned above, rib gaps seen in CCMS appears to locate around the angle of the rib at the epaxial-hypaxial border (Doyle, 1969, Silverman et al., 1980, Tachibana et al., 1980, Plotz et al., 1996, Watson et al., 2014, Tooley et al., 2016). The shaft defects observed through Wnt inhibition in this study occurred in a similar position to CCMS, with both the epaxial and hypaxial domains preserved (Fig. 1B,C; Fig. 2A-D). However, in the experiment the gaps tended to be wider with PNU-74654 as opposed to Dkk1 (Fig. 2C,D). This could be due to the difference in the stability between the Wnt inhibitors, as observed between K02288 and BMP4. The chemical compound, PNU-74654, is likely more stable than the Dkk1 protein and hence retained for longer in the developing tissue where it continues to inhibit chondrogenesis for an extended period, resulting in larger gaps than that caused by Dkk1.

Somites are well-studied structures and known to be patterned dorsoventrally and mediolaterally, by signals emanating from the surrounding tissues (Bothe et al., 2007). Ventralisation of the somite occurs before segmentation and hence specifies the sclerotome. Whereas, mediolateral patterning occurs later in development and relies on Wnt and BMP to confer epaxial-hypaxial cell commitment (Cheng et al., 2004, Ahmed et al., 2006). Due to the distance from Wnt and BMP sources, sclerotome cells on the epaxial-hypaxial border are likely

susceptible to these reduced signals and may fail to undergo chondrogenic differentiation. It is postulated that this signal perturbation affects susceptible cells in the somite and may explain the position of the rib gap at the epaxial-hypaxial boundary, both experimentally and in CCMS.

Chondrogenesis

The relationship between the Wnt and BMP pathways in cartilage formation are highly complex and, unlike in osteogenesis, the developmental steps of chondrogenesis have not been well defined. In particular, there has been much discussion in the literature as to whether the Wnt pathway is a positive or negative regulator of chondrocyte differentiation and proliferation (Tuan, 2003, Akiyama et al., 2004, Chen et al., 2007, Dao et al., 2012). *In vitro* studies using the mesenchymal cell line C3H10T1/2 have shown that BMP2 strongly promotes chondrocyte differentiation and that Wnt enhances this (Fischer et al., 2002). Moreover, mouse *in vivo* studies also show that the Wnt pathway promotes chondrocyte differentiation and Sox9 expression in the presence of BMP2, showing that the Wnt pathway is a positive regulator of chondrogenesis (Yano et al., 2005, Chen et al., 2007). This may explain how inhibition of the Wnt pathway in this study blocked cartilage formation in the presence of endogenous BMPs.

The radiolucent space in the rib gaps in CCMS is filled by fibrous tissues *in vivo* (Silverman et al., 1980, Oestreich and Stanek, 2010). In this study, a fibrous translucent tissue was also seen to bridge the rib gap. It is speculated that the cells which failed to differentiate into chondrocytes had adopted the tenocyte lineage, loosely connecting the proximal and distal parts of the rib, as seen in Fig. 2D.

476

477 **The effect of the BMP and Shh pathways on skeletal development**

478 In contrast to somite patterning and sclerotome induction that require BMP
479 antagonism by Noggin (McMahon et al., 1998), differentiation of the sclerotome
480 to undergo chondrogenesis requires BMP signals. Together with Shh, BMP
481 signals establish an autoregulatory loop of *Sox9* and *Nkx3.2*, two genes essential
482 for chondrogenesis (Zeng et al., 2002). Because of this, over-expression of
483 Noggin in already-formed somites results in loss of ribs and vertebrae (Murtaugh
484 et al., 1999), reflected in our results with K02288 (Fig. 4). Reducing BMP signals
485 by heterozygous deletion of BMP2 and 4 shows a milder yet similar phenotype,
486 in which only the proximal part of the last rib fails to form (Goldman et al., 2009,
487 Goldman et al., 2006). Due to the opposing roles of the BMP pathway in somite
488 patterning and chondrogenesis for the cartilage development, phenotypes
489 caused by BMP4 and K02288 resulted in similar phenotypes as discussed above.
490 Given the instructive role of Shh in sclerotome induction, one might anticipate
491 that the Shh inhibitor cyclopamine would cause a drastic phenotype on the
492 skeletal development. In fact, targeted deletion of *Shh* in mouse results in an
493 almost complete lack of axial skeleton (Chiang et al., 1996). However,
494 cyclopamine does not affect already-formed somites (Incardona et al., 1998),
495 suggesting that the ventral part of paraxial mesoderm is committed to form the
496 sclerotome at a very early stage by endogenous Shh before bead implantation.
497 As such, the fate of the ventral mesoderm to form the sclerotome could not be
498 altered in this study, which also explains why blocking BMP signals by K02288
499 did not enhance the effect of endogenous Noggin that would otherwise have
500 yielded extra-cartilage phenotypes.

Conclusion

Here we show that local modulation of the Wnt and BMP pathways produces marked axial skeletal abnormalities. The rib gap defect, which is pathognomonic of CCMS, as well as the missing rib and shortened rib defects, were recapitulated in this study. Particularly, the shaft defect has never before been seen in any mouse mutants or other model animals to our knowledge. The proposed mechanism of action postulates that there is a susceptive area in the dorsal sclerotome at the epaxial-hypaxial boundary, that is particularly vulnerable to the balance of signals during somite patterning. With reduced Wnt pathway activity, these cells are no longer able to differentiate into chondrocytes, hence yielding rib gaps. An intriguing question is why the phenotype is so localised in CCMS patients, despite the fact that both the Wnt and BMP pathways are required in many other regions during embryogenesis. The fact that basic developmental steps of embryogenesis which require Wnt and BMP, such as axial elongation and visceral development, are largely normal in CCMS patients, shows that the global effect on pathway activities is minimal. Consequently, only the structures requiring a precise level of the signalling activities can be affected.

Acknowledgments

We thank Dr M. Cheung for *Sox9* probe and Miss S. Jain for technical assistance with Figure 6.

Funding was through University of Bristol, INSPIRE and the Dick Smith Fund. The funding bodies had no input in the design of the study, collection, analysis or interpretation of data.

The authors declare that they have no competing interests. Further data can be obtained from the authors upon request.

Authors' contributions

BT conducted the experiments, photographed the embryos, reported and analysed the results and was a major contributor in writing the manuscript. NI conducted the pilot experiments, curated the hypothesis, designed the experiments, helped to analyse the data and was also a major contributor to writing the manuscript.

References

Acloque H, Wilkinson DG, Nieto MA (2008) In situ hybridization analysis of chick embryos in whole-mount and tissue sections. *Methods Cell Biol,* **87,** 169-85.

Ahmed MU, Cheng L, Dietrich S (2006) Establishment of the epaxial-hypaxial boundary in the avian myotome. *Dev Dyn,* **235,** 1884-94.

Akiyama H, Lyons JP, Mori-Akiyama Y, et al. (2004) Interactions between Sox9 and beta-catenin control chondrocyte differentiation. *Genes Dev,* **18,** 1072-87.

Bacrot S, Doyard M, Huber C, et al. (2015) Mutations in SNRPB, encoding components of the core splicing machinery, cause cerebro-costo-mandibular syndrome. *Hum Mutat,* **36,** 187-90.

Balling R, Deutsch U, Gruss P (1988) undulated, a mutation affecting the development of the mouse skeleton, has a point mutation in the paired box of Pax 1. *Cell,* **55,** 531-5.

Behringer R (2014) *Manipulating the mouse embryo : a laboratory manual*.

Bothe I, Ahmed MU, Winterbottom FL, von Scheven G, Dietrich S (2007) Extrinsic versus intrinsic cues in avian paraxial mesoderm patterning and differentiation. *Dev Dyn,* **236,** 2397-409.

Brand-Saberi B, Ebensperger C, Wilting J, Balling R, Christ B (1993) The ventralizing effect of the notochord on somite differentiation in chick embryos. *Anat Embryol (Berl),* **188,** 239-45.

Brent AE, Schweitzer R, Tabin CJ (2003) A somitic compartment of tendon progenitors. *Cell,* **113,** 235-48.

Cairns DM, Sato ME, Lee PG, Lassar AB, Zeng L (2008) A gradient of Shh establishes mutually repressing somitic cell fates induced by Nkx3.2 and Pax3. *Dev Biol,* **323,** 152-65.

Capdevila J, Tabin C, Johnson RL (1998) Control of dorsoventral somite patterning by Wnt-1 and beta-catenin. *Dev Biol,* **193,** 182-94.

Chen Y, Whetstone HC, Youn A, et al. (2007) Beta-catenin signaling pathway is crucial for bone morphogenetic protein 2 to induce new bone formation. *J Biol Chem,* **282,** 526-33.

Cheng L, Alvares LE, Ahmed MU, El-Hanfy AS, Dietrich S (2004) The epaxial-hypaxial subdivision of the avian somite. *Dev Biol,* **274,** 348-69.

Chiang C, Litingtung Y, Lee E, et al. (1996) Cyclopia and defective axial patterning in mice lacking Sonic hedgehog gene function. *Nature,* **383,** 407-13.

Christ B, Huang R, Scaal M (2004) Formation and differentiation of the avian sclerotome. *Anat Embryol (Berl),* **208,** 333-50.

Dao DY, Jonason JH, Zhang Y, et al. (2012) Cartilage-specific beta-catenin signaling regulates chondrocyte maturation, generation of ossification centers, and perichondrial bone formation during skeletal development. *J Bone Miner Res,* **27,** 1680-94.

Dietrich S, Gruss P (1995) undulated phenotypes suggest a role of Pax-1 for the development of vertebral and extravertebral structures. *Dev Biol,* **167,** 529-48.

Doyle JF (1969) The skeletal defects of the cerebro-costo-mandibular syndrome. *Ir J Med Sci,* **8,** 595-603.

Evans DJ (2003) Contribution of somitic cells to the avian ribs. *Dev Biol,* **256,** 114-26.

Fan CM, Tessier-Lavigne M (1994) Patterning of mammalian somites by surface ectoderm and notochord: evidence for sclerotome induction by a hedgehog homolog. *Cell,* **79,** 1175-86.

583 Fischer L, Boland G, Tuan RS (2002) Wnt-3A enhances bone morphogenetic protein-2-
584 mediated chondrogenesis of murine C3H10T1/2 mesenchymal cells. *J Biol Chem,*
585 **277,** 30870-8.
586 Furumoto TA, Miura N, Akasaka T, et al. (1999) Notochord-dependent expression of
587 MFH1 and PAX1 cooperates to maintain the proliferation of sclerotome cells
588 during the vertebral column development. *Dev Biol,* **210,** 15-29.
589 Geetha-Loganathan P, Nimmagadda S, Scaal M, Huang R, Christ B (2008) Wnt signaling
590 in somite development. *Ann Anat,* **190,** 208-22.
591 Goldman DC, Donley N, Christian JL (2009) Genetic interaction between Bmp2 and
592 Bmp4 reveals shared functions during multiple aspects of mouse organogenesis.
593 *Mech Dev,* **126,** 117-27.
594 Goldman DC, Hackenmiller R, Nakayama T, et al. (2006) Mutation of an upstream
595 cleavage site in the BMP4 prodomain leads to tissue-specific loss of activity.
596 *Development,* **133,** 1933-42.
597 Hamburger V, Hamilton HL (1951) A series of normal stages in the development of the
598 chick embryo. *Journal of Morphology,* **88,** 49-92.
599 Holmen SL, Zylstra CR, Mukherjee A, et al. (2005) Essential role of beta-catenin in
600 postnatal bone acquisition. *J Biol Chem,* **280,** 21162-8.
601 Huang R, Stolte D, Kurz H, et al. (2003) Ventral axial organs regulate expression of
602 myotomal Fgf-8 that influences rib development. *Dev Biol,* **255,** 30-47.
603 Huang R, Zhi Q, Schmidt C, Wilting J, Brand-Saberi B, Christ B (2000) Sclerotomal
604 origin of the ribs. *Development,* **127,** 527-32.
605 Ikeya M, Takada S (1998) Wnt signaling from the dorsal neural tube is required for the
606 formation of the medial dermomyotome. *Development,* **125,** 4969-76.
607 Incardona JP, Gaffield W, Kapur RP, Roelink H (1998) The teratogenic Veratrum
608 alkaloid cyclopamine inhibits sonic hedgehog signal transduction. *Development,*
609 **125,** 3553-62.
610 Itasaki N, Hoppler S (2010) Crosstalk between Wnt and bone morphogenic protein
611 signaling: a turbulent relationship. *Dev Dyn,* **239,** 16-33.
612 Johnson RL, Laufer E, Riddle RD, Tabin C (1994) Ectopic expression of Sonic hedgehog
613 alters dorsal-ventral patterning of somites. *Cell,* **79,** 1165-73.
614 Koseki H, Wallin J, Wilting J, et al. (1993) A role for Pax-1 as a mediator of notochordal
615 signals during the dorsoventral specification of vertebrae. *Development,* **119,** 649-
616 60.
617 Lefebvre V, Huang W, Harley VR, Goodfellow PN, de Crombrugghe B (1997) SOX9 is
618 a potent activator of the chondrocyte-specific enhancer of the pro alpha1(II)
619 collagen gene. *Mol Cell Biol,* **17,** 2336-46.
620 Lynch DC, Revil T, Schwartzentruber J, et al. (2014) Disrupted auto-regulation of the
621 spliceosomal gene SNRPB causes cerebro-costo-mandibular syndrome. *Nat*
622 *Commun,* **5,** 4483.
623 Mao B, Wu W, Li Y, et al. (2001) LDL-receptor-related protein 6 is a receptor for
624 Dickkopf proteins. *Nature,* **411,** 321-5.
625 Marcelle C, Stark MR, Bronner-Fraser M (1997) Coordinate actions of BMPs, Wnts, Shh
626 and noggin mediate patterning of the dorsal somite. *Development,* **124,** 3955-63.
627 Mbalaviele G, Sheikh S, Stains JP, et al. (2005) Beta-catenin and BMP-2 synergize to
628 promote osteoblast differentiation and new bone formation. *J Cell Biochem,* **94,**
629 403-18.
630 McKeown SJ, Lee VM, Bronner-Fraser M, Newgreen DF, Farlie PG (2005) Sox10
631 overexpression induces neural crest-like cells from all dorsoventral levels of the
632 neural tube but inhibits differentiation. *Dev Dyn,* **233,** 430-44.

McMahon JA, Takada S, Zimmerman LB, Fan CM, Harland RM, McMahon AP (1998) Noggin-mediated antagonism of BMP signaling is required for growth and patterning of the neural tube and somite. *Genes Dev,* **12,** 1438-52.
Meijer L, Skaltsounis AL, Magiatis P, et al. (2003) GSK-3-selective inhibitors derived from Tyrian purple indirubins. *Chem Biol,* **10,** 1255-66.
Moore KL, Dalley II AF, Agur AMR (2014) *Clinically oriented anatomy,* Lippincott Williams & Wilkins, Baltimore, USA.
Muller TS, Ebensperger C, Neubuser A, et al. (1996) Expression of avian Pax1 and Pax9 is intrinsically regulated in the pharyngeal endoderm, but depends on environmental influences in the paraxial mesoderm. *Dev Biol,* **178,** 403-17.
Murtaugh LC, Chyung JH, Lassar AB (1999) Sonic hedgehog promotes somitic chondrogenesis by altering the cellular response to BMP signaling. *Genes Dev,* **13,** 225-37.
Nifuji A, Kellermann O, Kuboki Y, Wozney JM, Noda M (1997) Perturbation of BMP signaling in somitogenesis resulted in vertebral and rib malformations in the axial skeletal formation. *J Bone Miner Res,* **12,** 332-42.
Oestreich AE, Stanek JW (2010) Preautopsy imaging in cerebro-costo-mandibular syndrome. *Pediatr Radiol,* **40 Suppl 1,** S50.
Olivera-Martinez I, Coltey M, Dhouailly D, Pourquie O (2000) Mediolateral somitic origin of ribs and dermis determined by quail-chick chimeras. *Development,* **127,** 4611-7.
Otto A, Schmidt C, Patel K (2006) Pax3 and Pax7 expression and regulation in the avian embryo. *Anat Embryol (Berl),* **211,** 293-310.
Pan Q, Yu Y, Chen Q, et al. (2008) Sox9, a key transcription factor of bone morphogenetic protein-2-induced chondrogenesis, is activated through BMP pathway and a CCAAT box in the proximal promoter. *J Cell Physiol,* **217,** 228-41.
Peters H, Wilm B, Sakai N, Imai K, Maas R, Balling R (1999) Pax1 and Pax9 synergistically regulate vertebral column development. *Development,* **126,** 5399-408.
Plotz FB, van Essen AJ, Bosschaart AN, Bos AP (1996) Cerebro-costo-mandibular syndrome. *Am J Med Genet,* **62,** 286-92.
Pourquie O, Fan CM, Coltey M, et al. (1996) Lateral and axial signals involved in avian somite patterning: a role for BMP4. *Cell,* **84,** 461-71.
Qian L, Mahaffey JP, Alcorn HL, Anderson KV (2011) Tissue-specific roles of Axin2 in the inhibition and activation of Wnt signaling in the mouse embryo. *Proc Natl Acad Sci U S A,* **108,** 8692-7.
Saltzman AL, Pan Q, Blencowe BJ (2011) Regulation of alternative splicing by the core spliceosomal machinery. *Genes Dev,* **25,** 373-84.
Sanvitale CE, Kerr G, Chaikuad A, et al. (2013) A new class of small molecule inhibitor of BMP signaling. *PLoS One,* **8,** e62721.
Semenov MV, Tamai K, Brott BK, Kuhl M, Sokol S, He X (2001) Head inducer Dickkopf-1 is a ligand for Wnt coreceptor LRP6. *Curr Biol,* **11,** 951-61.
Silverman FN, Strefling AM, Stevenson DK, Lazarus J (1980) Cerebro-costo-mandibular syndrome. *J Pediatr,* **97,** 406-16.
Smith DW, Theiler K, Schachenmann G (1966) Rib-gap defect with micrognathia, malformed tracheal cartilages, and redundant skin: a new pattern of defective development. *J Pediatr,* **69,** 799-803.

Stafford DA, Brunet LJ, Khokha MK, Economides AN, Harland RM (2011) Cooperative activity of noggin and gremlin 1 in axial skeleton development. *Development,* **138,** 1005-14.

Stafford DA, Monica SD, Harland RM (2014) Follistatin interacts with Noggin in the development of the axial skeleton. *Mech Dev,* **131,** 78-85.

Stern CD, Keynes RJ (1987) Interactions between somite cells: the formation and maintenance of segment boundaries in the chick embryo. *Development,* **99,** 261-72.

Tachibana K, Yamamoto Y, Osaki E, Kuroki Y (1980) Cerebro-costo-mandibular syndrome. A case report and review of the literature. *Hum Genet,* **54,** 283-6.

Tonegawa A, Funayama N, Ueno N, Takahashi Y (1997) Mesodermal subdivision along the mediolateral axis in chicken controlled by different concentrations of BMP-4. *Development,* **124,** 1975-84.

Tonegawa A, Takahashi Y (1998) Somitogenesis controlled by Noggin. *Dev Biol,* **202,** 172-82.

Tooley M, Lynch D, Bernier F, et al. (2016) Cerebro-Costo-Mandibular syndrome: Clinical, Radiological and Genetic Findings. *American Journal of Medical Genetics,* **170,** 1115-26.

Trosset JY, Dalvit C, Knapp S, et al. (2006) Inhibition of protein-protein interactions: the discovery of druglike beta-catenin inhibitors by combining virtual and biophysical screening. *Proteins,* **64,** 60-7.

Tuan RS (2003) Cellular signaling in developmental chondrogenesis: N-cadherin, Wnts, and BMP-2. *J Bone Joint Surg Am,* **85-A Suppl 2,** 137-41.

Wallin J, Wilting J, Koseki H, Fritsch R, Christ B, Balling R (1994) The role of Pax-1 in axial skeleton development. *Development,* **120,** 1109-21.

Watson TA, Arthurs OJ, Muthialu N, Calder AD (2014) Multi-detector thoracic CT findings in cerebro-costo-mandibular syndrome: rib gaps and failure of costo-vertebral separation. *Skeletal Radiol,* **43,** 263-6.

Wozney JM, Rosen V, Celeste AJ, et al. (1988) Novel regulators of bone formation: molecular clones and activities. *Science,* **242,** 1528-34.

Yano F, Kugimiya F, Ohba S, et al. (2005) The canonical Wnt signaling pathway promotes chondrocyte differentiation in a Sox9-dependent manner. *Biochem Biophys Res Commun,* **333,** 1300-8.

Yoon BS, Lyons KM (2004) Multiple functions of BMPs in chondrogenesis. *J Cell Biochem,* **93,** 93-103.

Zeng L, Kempf H, Murtaugh LC, Sato ME, Lassar AB (2002) Shh establishes an Nkx3.2/Sox9 autoregulatory loop that is maintained by BMP signals to induce somitic chondrogenesis. *Genes Dev,* **16,** 1990-2005.

720 **Figure Legends**

721 **Fig. 1 Phenotypes by Dkk1**

722 Alcian-blue stained chick embryos at HH stage 32-33, dorsal view, following
723 implantation of Dkk1 beads (yellow). Red arrows indicate the phenotype. The
724 right column (A'-H') shows higher magnifications of the phenotypic area, with
725 dotted lines indicating missing rib parts. Beads are highlighted in yellow in low
726 magnification figures where possible. Chickens normally have seven pairs of ribs.
727 Scale bar, 1 mm.
728 **A**) Large posterior proximal defects of the fourth and fifth ribs on the left and the
729 fourth, sixth and seventh ribs on the right.
730 **B**) Shaft defect in the second right rib
731 **C**) Shaft defects of the first and second left ribs. A bead is noted inferior to distal
732 rib segment.
733 **D**) Proximal defects of the first left and third right ribs, with severe fusion and
734 malformation of vertebrae T1-T7.
735 **E**) Missing third and fifth right ribs with a shortened second left rib, as well as
736 malformation of vertebrae T2-T5.
737 **F**) Missing sixth right rib and seventh left rib, with an additional eighth rib.
738 **G**) Missing fifth right rib.
739 **H**) Missing seventh right rib.
740
741

742 **Fig. 2 Phenotypes by PNU-74654**

743 Alcian-blue stained chick embryos at HH stage 32-33 (**A-C,** and **E-G)** and Alcian-
744 blue plus Alizarin-red stained 35-36 (**D,H**), dorsal view. Red arrows and

arrowheads indicate the phenotype. Beads are highlighted in yellow. The right column (A'-H') shows higher magnifications of the phenotypic area, with dotted lines indicating missing rib parts. Beads are highlighted in yellow in low magnification figures where possible. Scale bar, 1 mm.

A) Shaft defect of fourth right rib. Beads are noted in the plane of the second and fourth right ribs.

B) Shaft defect of seventh left rib. Asterisk indicates mechanical damage to seventh right rib.

C) Large posterior shaft defect of fifth left rib.

D) Large posterior shaft defect on the third right rib. The proximal part of the third rib is seen adjacent to the vertebral body and translucent tissue is seen in the gap *in situ*.

E) Bilateral missing seventh ribs and small proximal defect of third right rib (arrows). Some ectopic cartilage deposition is noted in the fifth left and right ribs. A bead is noted medial to the third right rib head.

F) Missing seventh ribs bilaterally and proximal defect of the fifth left rib. The fourth left and right ribs are malformed and there is bifurcation of the third right rib.

G) Proximal defect of fourth rib.

H) Missing sixth right rib.

Fig. 3 Phenotypes by BMP4

Alcian-blue stained chick embryos at HH stage 32-33, dorsal view. Red arrows and arrowheads indicate the phenotype. The right column (A'-H') shows higher

769 magnifications of the phenotypic area, with dotted lines indicating missing rib
770 parts. Scale bar, 1 mm.
771 **A**) Multiple missing and shortened ribs. Scoliosis is noted as well as fusion and
772 deformity of vertebrae T3-T7.
773 **B**) Missing second, third, fifth and sixth right ribs with only shortened remnants of
774 the first, fourth and seventh ribs. There is malformation of vertebrae T2-T6.
775 **C**) Missing fifth left rib and scoliosis. Fusion and malformation of vertebrae T4-
776 T7. Fusion of left sixth and seventh ribs are indicated by arrowhead.
777 **D**) Missing first, second and third ribs bilaterally as well as missing fourth right rib
778 and shortened fifth right rib. There is a hemi vertebral deformity of T1-T5 and
779 ectopic cartilage deposition.
780 **E**) Proximal defect of sixth right rib.
781 **F**) Vertebral defects and fusion of T4-T6 causing a reduced amount of cartilage
782 deposition in the form of the fifth rib with shaft defect (arrow) and the rib inferior
783 to this, presumably the fifth rib, is then attached to T6 along with the sixth rib. An
784 eighth rib pair is noted. Fusion and branching are also noted at the distal ends
785 (arrowhead).
786 **G)** Missing fourth right rib and shortened fifth left rib (arrow). Fusion of the third
787 and fourth ribs on the right (arrowhead).
788 **H)** The vertebral column is fused from T1-T7 and the fifth right rib is separated
789 from its vertebral origin but fused to the proximal end of the fourth rib to create a
790 bifurcated appearance.

791

792 **Fig. 4 Phenotypes by K02288.**

Alcian-blue stained chick embryos at HH stage 32-33, dorsal view. Red arrows and arrowhead indicate the phenotype. The right column (A'-H') shows higher magnifications of the phenotypic area, with dotted lines indicating missing rib parts. Beads are highlighted in yellow in low magnification figures where possible. Scale bar, 1 mm.

A) Proximal defect of third right rib which has become fused proximally to the fourth rib. An ectopic eighth rib pair is present and a bead is seen superior to the second rib.

B) Fusion of the fourth and fifth ribs bilaterally to create a bifurcated appearance. Vertebrae T4-T5 are fused. Asterisk indicates mechanical damage. An additional pair of eighth ribs are seen, with the one on the right side is fused to the seventh.

C) Missing fourth left rib and fusion of the proximal end of the fourth right rib to the third rib. Vertebrae T3 and T4 are fused. A bead is noted medially in the fused T3 and T4.

D) Complete fusion of the third and fourth right ribs to form a single rib with a superior point of attachment to the second rib.

E) Missing fourth left rib and seventh right rib. There is malformation of vertebrae T4 and T6-T7.

F) Shortened sixth right rib with distal sixth and seventh rib fusion (arrowhead).

G) Fusion of T1 and T2.

H) Fusion of T6 and T7 with a small degree of malformation of T6. Asterisk indicates mechanical damage.

Fig. 5 Phenotypes by cyclopamine, BIO and DMSO.

Alcian-blue stained chick embryos at HH stage 32-33, dorsal view. (**A-B)**, cyclopamine; **(C-D)**, BIO; **(E-F)**, DMSO. Beads are highlighted in yellow in low magnification figures where possible. Red arrows indicate the phenotype. Scale bar, 1 mm.

A) Fusion of the fifth and sixth left ribs as well as fusion and malformation of T5 and T6.

B) Vertebral bridging.

C) Fusion of the fourth right rib to the proximal end of the fifth rib which is malformed through thickening proximally.

D) Malformation of the sixth right rib, with distortion towards the bead inferiorly.

E) Bifurcation of the sixth left rib.

F) A normal set of seven ribs.

Fig. 6 Expression of *Sox9* in bead-implanted embryos.

A-**F**) Transverse sections of *Sox9*-stained embryos 24 hours after bead implantation at the level of somites 20-26, with pathway modulator indicated. The left panel shows the section containing the bead, while the right panel shows the adjacent section. The open neural tube seen in A and B reflects the fragility of the young neural tube.

Control DMSO beads show no effect on *Sox9* expression (**a**) whereas **b**-**d**) show reduced staining on the ipsilateral side to implantation. Scale bar, 100 μm.

Table 1. Chemicals and proteins used for bead implantation in this study

Chemical/ Protein	Full Name	Concentration	Pathway Affected	Mechanism
DMSO	Dimethyl Sulphoxide	100%	Solvent/ control	Solvent vehicle for BIO, Cyclopamine, K02288 and PNU-74654
PBS	Phosphate-Buffered Saline	1x	Solvent/ control	Solvent for proteins BMP4 and Dkk1
Dkk1	Dickkopf-related protein 1	0.5 mg/ml	Wnt inhibitor	Wnt pathway inhibitor by antagonism of LRP5/6 receptors preventing Wnt signal transduction (Mao et al., 2001, Semenov et al., 2001)
PNU-74654	Benzoic acid, 2-phenoxy-, 2-[(5-methyl-2-furanyl) methylene]hydrazide	50 mM	Wnt inhibitor	Wnt pathway inhibitor through disruption of the Tcf4-β-catenin complex that is essential for signal transduction (Trosset et al., 2006)
BIO	6-bromoindirubin-3'-oxime	5 mM	Wnt activator	GSK3 inhibitor, activating the Wnt pathway via inhibiting GSK3β (Meijer et al., 2003)
BMP4	Bone Morphogenic Protein 4	0.1 mg/ml	BMP activator	Ligand of type I and II BMP receptors (Wozney et al., 1988)
K02288	(3-[6-amino-5-(3,4,5-trimethoxy-phenyl)-pyridin-3-yl]-phenol)	1.5 mM	BMP inhibitor	Small molecule inhibitor of the BMP receptor kinase ALK2 (Sanvitale et al., 2013)
Cyclopamine	11-Deoxyjervine	20 mM	Shh inhibitor	Small molecule alkaloid inhibitor of hedgehog signalling through direct antagonism of smoothened, the Shh receptor (Incardona et al., 1998)

Table 2. Result of statistical analyses of each chemical against the phenotypes produced by two bead implantation

	Rib Gap		Missing ribs §	Scoliosis	Short ribs §	Bifurcated Rib	Rib fusion	Malformed rib	Vertebral malformation	Vertebral bridge	Vertebral fusion	Ectopic cartilage	Additional rib	Phenotype shown
	Shaft defect §	Proximal rib defect		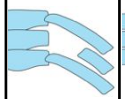	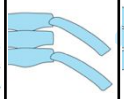	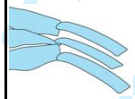		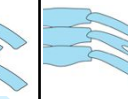	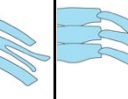	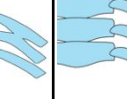	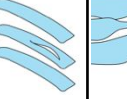			
Controls (n=29)	0	0	1	0	0	2	1	0	2	4	1	12	2	16 (55%)
DKK-1 (n=23)	4**	4**	7**	1	2	1	3	2	7*	0	4	3	1	15 (65%)
PNU-74654 (n=17)	3*	4*	4	0	0	3	2	1	4	1	4	7	4	15 (88%)
BIO (n=7)	0	1	1	0	0	1	1	2*	1	0	0	0	0	7 (100%)
BMP4 (n=14)	0	2	6**	3*	3*	2	4*	3*	8***	0	7***	1	1	11 (79%)
K02288 (n=10)	0	1	4*	0	1	2	5**	1	5**	1	6***	1	0	8 (80%)
CYC (n=16)	0	0	1	0	1	2	2	2	3	3	4	7	0	11 (69%)

Significance level is indicated by * (P<0.05), ** (P<0.01), *** (P<0.001).

§ indicates phenotypic features typical of CCMS.

Each embryo can be counted in more than one column.

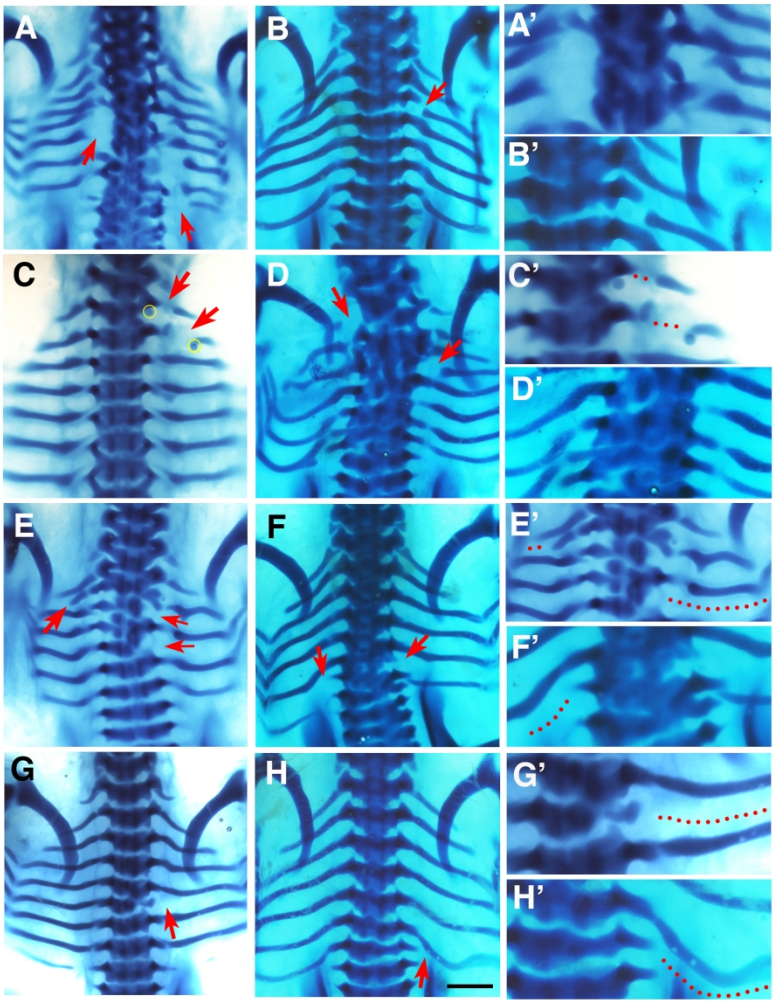

Figure 1

Fig. 1

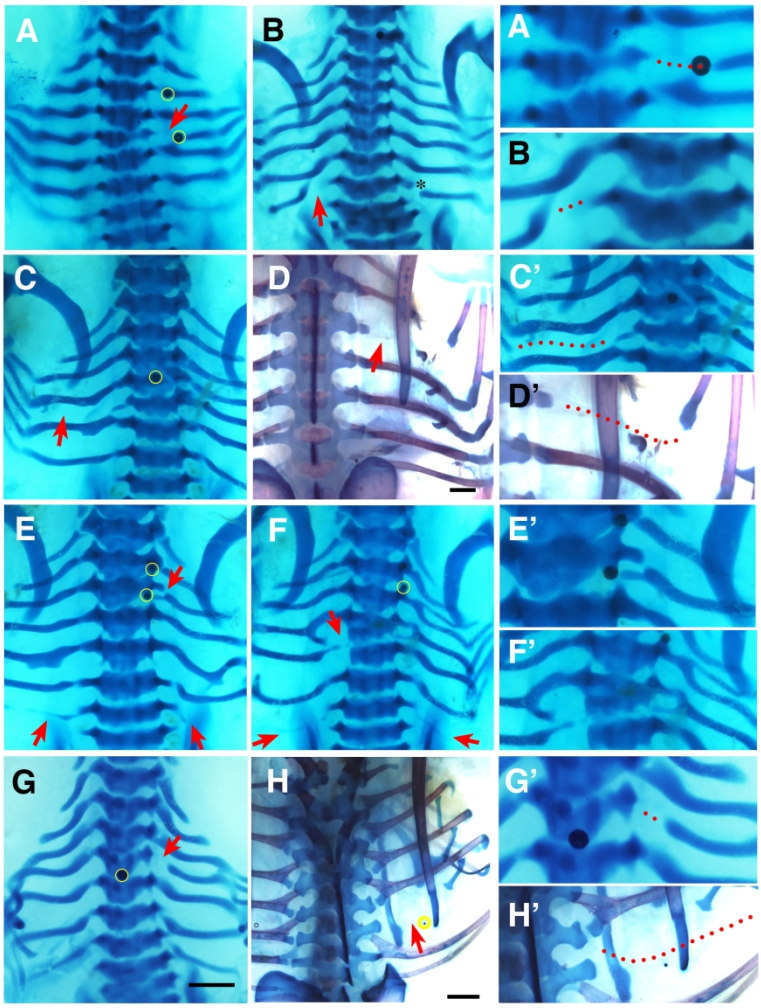

Figure 2

Fig. 2

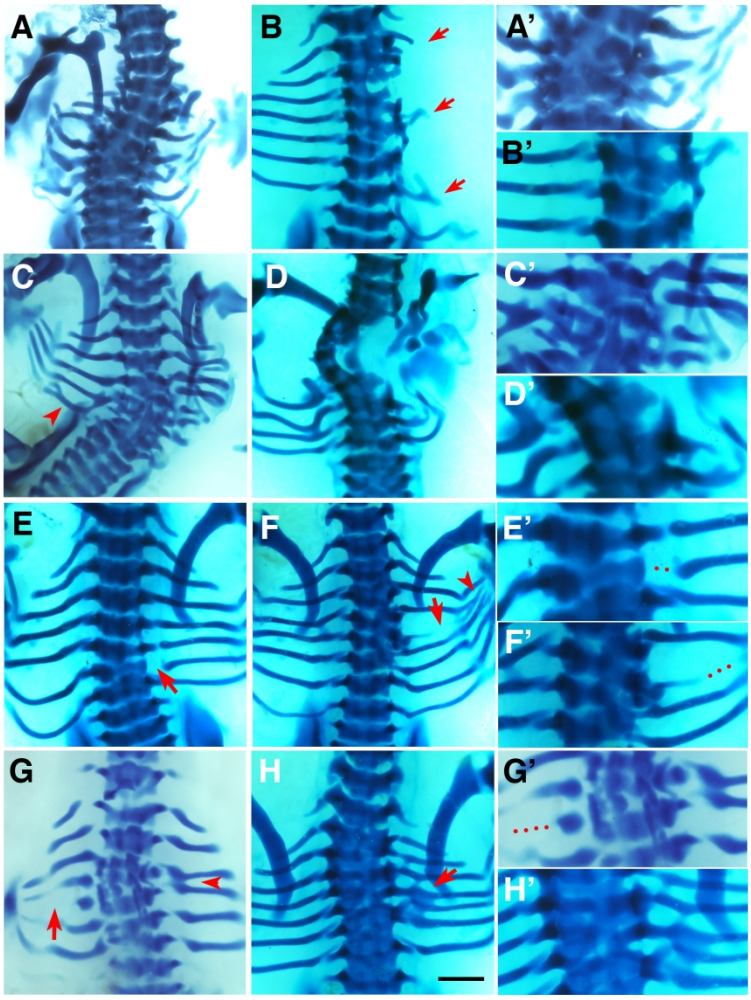

Figure 3

Fig. 3

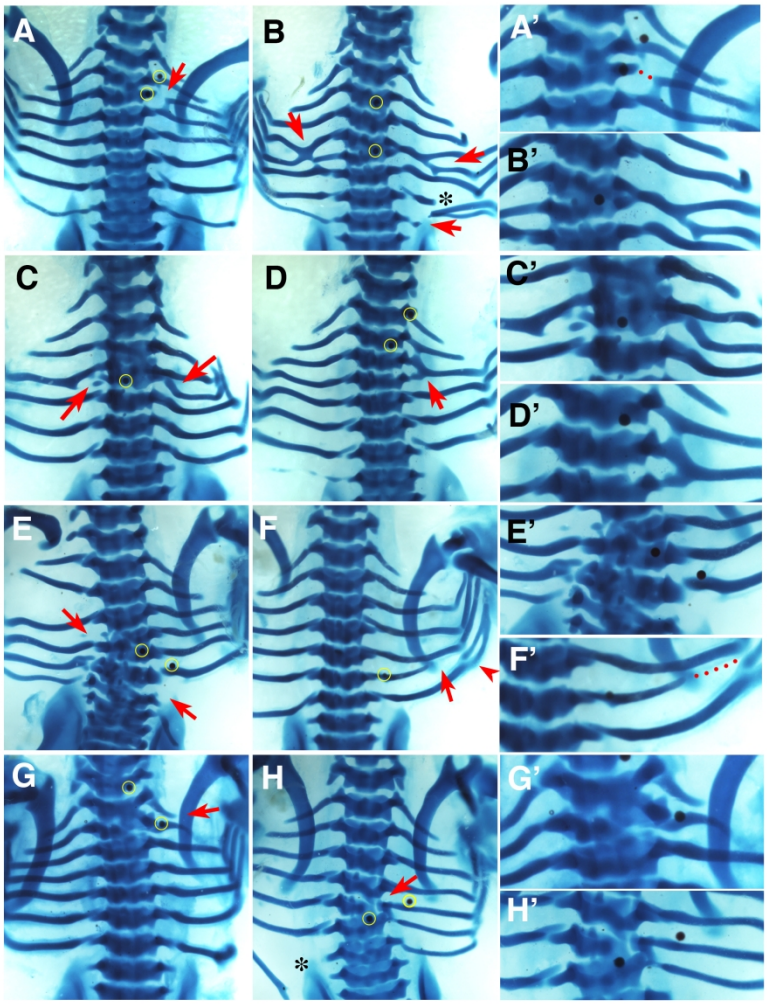

Figure 4

Fig. 4

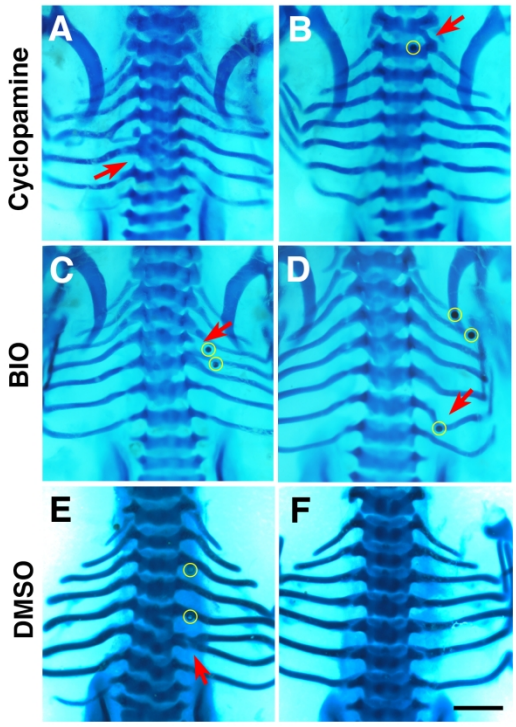

Figure 5

Fig. 5

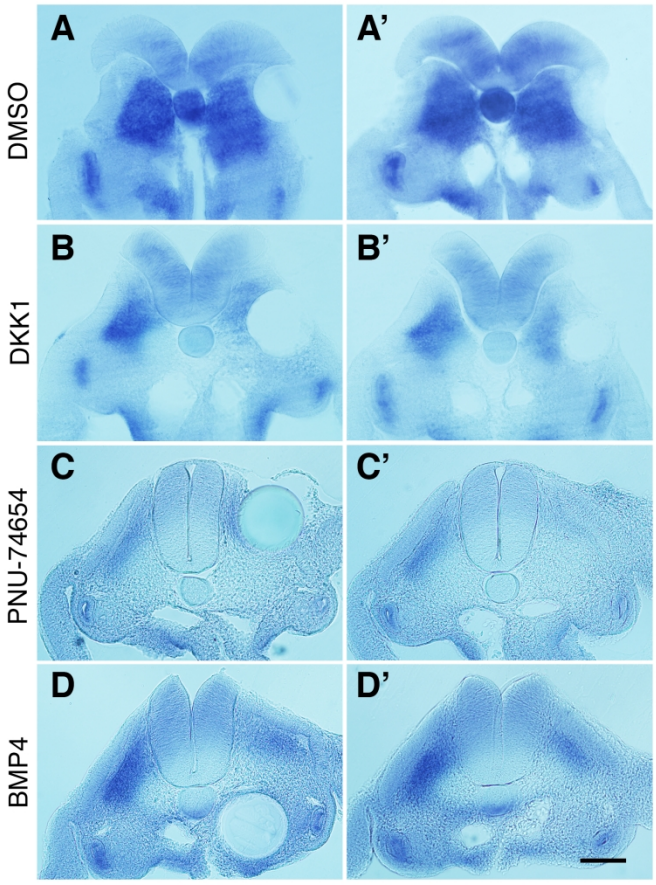

Figure 6

Fig 6